Neutrino energy reconstruction from one-muon and one-proton events

Andrew P. Furmanski and Jan T. Sobczyk

Phys. Rev. C **95**, 065501 — Published 5 June 2017

DOI: 10.1103/PhysRevC.95.065501

Neutrino energy reconstruction from one muon and one proton events

Andrew P. Furmanski[1] and Jan T. Sobczyk[2]

[1] *The University of Manchester, Oxford Road, Manchester, M13 9PL, UK*
[2] *Institute of Theoretical Physics, University of Wrocław, pl. M. Borna 9, 50-204, Wrocław, Poland*

(Dated: May 11, 2017)

We propose a method of selecting a high purity sample of charged current quasi-elastic neutrino interactions to obtain a precise reconstruction of the neutrino energy. The performance of the method was verified with several tests using GENIE, NEUT and NuWro Monte Carlo event generators with both carbon and argon targets. The method can be useful in neutrino oscillation studies with beams of a few GeV.

I. INTRODUCTION

Neutrino oscillations occur as a function of neutrino energy and distance. A standard long-baseline experiment using two fixed-distance detectors therefore needs to be able to reconstruct the neutrino energy on an event-by-event basis in order to infer precise oscillation parameters. This is why in recent years there has been a lot of discussion of unbiased neutrino energy reconstruction based on particles detected in the final state after escaping the target nucleus. The topic is important because neutrino fluxes are never mono-energetic and even in an off-axis configuration have a significant spread. The discussion has became even more intense after realizing that in the few GeV energy region (where most current and planned long baseline oscillation experiments operate) there is a significant contribution from two-body current mechanism making the situation even more complicated [1–3]. For review articles see Ref. [4].

In the few GeV region the most common reaction, and one that is easy to study and identify due to its simple topology, is charged current quasi-elastic (CCQE) scattering. If we restrict ourselves for a moment to neutrino-nucleon scattering, the CCQE interaction is:

$$\nu_\mu \; n \to \mu^- \; p \tag{1}$$

$$\bar{\nu}_\mu \; p \to \mu^+ \; n. \tag{2}$$

In what follows, we focus on muon neutrinos only. In oscillation experiments targets are mostly nuclei. If the momentum and energy transferred to the hadronic system is large enough, one can rely on the impulse approximation (IA) [5] according to which interactions occur on individual (bound and moving) nucleons and the meaning of CCQE remains valid. This is confirmed by the clear observation of a QE peak in electron nucleus target inclusive cross section measurements [6]. In neutrino experiments, an analogous identification of the QE peak is impossible, because one does not know the amount of energy and momentum transferred to the nucleus on an event by event basis (for a recent attempt to estimate these quantities in neutrino experiment see Ref. [7]).

In the IA picture, neutrino scattering is a two step process where a primary interaction on a bound nucleon (or nucleon pair) is followed by hadron rescatterings called final state interactions (FSI). This is why neutrino experimental groups introduced the notion of CCQE-like events. They are defined as those with a muon and no mesons in the final state (i.e. $1\mu + 0\pi + X$, where X represents any number of nucleons). The advantage of this notion is that it is defined with no ambiguity and also it is relatively close to genuine CCQE in the IA picture. A widely discussed MiniBooNE measurement of the CCQE double differential cross section [1] was in fact a CCQE-like measurement after the results from tables VI and VIII in Ref. [1] are added. A more recent measurement of a CCQE-like cross section was reported by T2K [8]. In all cases, CCQE-like samples of events contain also those in which a real pion is first produced and then absorbed, and also those arising from a two-body mechanism, typically leading to two nucleon knock-out. Notice also that a true CCQE event will occasionally produce pions through FSI and thus not be classified as CCQE-like. A precise description of neutrino interactions in the few GeV energy region requires a careful combination of several dynamical models. This has been the motivation for numerous neutrino Monte Carlo (MC) event generators studies [9].

The goal of this paper is to propose a novel method to select high purity CCQE events out of CCQE-like experimental samples. The method works for events with exactly two particles detected in the final state: muon and proton. Muon identification is usually quite simple, however reconstructing the short tracks left by protons is more challenging. Nevertheless, in recent years experimental groups like T2K, MINERνA, ArgoNeuT have presented various studies using information from protons, see e.g. Ref. [10]. The ability to reconstruct a final state proton depends strongly on the details of the detector technique used. In segmented scintillators used by T2K in a near detector and by MINERvA a typical threshold for proton identification is $\sim$ 400 MeV/c. However, in liquid argon used in ArgoNeuT, MicroBooNE and proposed in the DUNE experiment the threshold is much lower: $\sim$ 200 MeV/c.

A sample with no mesons, exactly one muon and one proton consists of four basic categories of events: (i) CCQE events with a proton that did not suffer from FSI effects; (ii) CCQE events with a proton that at least once rescattered before was knocked-out and detected;

(iii) π production events with subsequent π absorption; (iv) two-body current events. The relative sizes of the contributions from these four categories depend on the neutrino beam spectrum, target nucleus and threshold for proton track identification. We propose a selection criteria which eliminates the vast majority of the events from categories (iii) and (iv) whilst keeping most of the events from categories (i) and (ii). The relative population of subsamples (i) and (ii) depends on the probability that a proton traverses the nucleus without interacting. This probability is often expressed as the nuclear transparency. Clearly, transparency depends on the nucleus size and is larger for carbon (about 60% [11]) than it is for argon. We are not aware of any proton transparency measurement for argon. More information on transparency studies for various targets can be found in Ref. [12].

It has been shown previously that the CCQE purity and energy resolution of a more exclusive $1\mu + 0\pi + 1p$ event sample are better than the more general $1\mu+0\pi+X$ sample [13], however we show here that further kinematic cuts can lead to significant improvements. From here on we refer to our sample of $1\mu+0\pi+1p$ events as CC0π1p. This sample is unambiguously defined, provided the proton detection threshold is known. Our argument is rather elementary and is based merely on energy and momentum conservation. If the event is indeed CCQE with no proton final state interactions, energy and momentum conservation allow one to resolve the kinematics of the process completely and calculate the initial neutrino and neutron three-momenta. Recently, various transverse kinematic studies were performed exploring momentum conservation in the plane perpendicular to the neutrino momentum vector [14]. In our computations we use also information from momentum conservation along the neutrino momentum vector. The obtained values of neutron momentum and neutrino energy should be almost exact for events from category (i). For the events from category (ii), the spread of the obtained values depends on the severity of the rescatterings experienced by the proton. For events from categories (iii) and (iv), our procedure is expected to produce largely random numbers. This is because the very assumption that the CCQE nteraction occurred on a neutron is not satisfied and the interaction mechanism is more complicated. This is confirmed by MC simulations. Appropriate cuts will be able to eliminate most of them.

As said before, the goal is to select true CCQE events. The target neutron momenta and separation energies can be realistically described by means of a spectral function (SF) [15]. The neutron momentum distribution consists of two parts: a mean field part dominating for $p < 250$ MeV/c and a correlation part responsible for the high momentum tail $p > 250$ MeV/c [16]. The mean field part can be understood in the language of the shell model [17]. The correlation part comes from short range correlated pairs. In the few GeV neutrino energy region the vast majority of CCQE events come from interactions on neutrons described by the mean field. Our selection aims to select those events by requiring a reconstructed neutron momentum of the order of ~ 250 MeV/c. In our computations we will have to estimate, on an event by event basis, the excitation energy of the remnant nucleus after a proton was knocked out. The estimation will be consistent with the assumption that we select mean field neutrons. Relevant information will be given in terms of removal energy from neutron energy levels.

Our main result is that the performance of the proposed selection method is indeed very good. We did numerical computations using three different MC event generators: GENIE [18], NEUT [19] and NuWro [20]. Each treats nuclear effects and, in particular, FSI effects in different way, yet the conclusions we obtained are quite similar. Thus we infer that a high purity CCQE sample of events can be obtained. For the selected sample we show that the precision of the energy reconstruction is extremely good, and outperforms other available methods.

Our paper is organized as follows. In Sect. II we present a framework in which the neutron momentum and neutrino energy are evaluated. In Sect. III we demonstrate the performance of the proposed method. We will discuss several examples using MiniBooNE [21], T2K (off-axis) [22], and NuMI (low-energy tune on-axis) [23] ν_μ fluxes with interactions occurring on carbon or argon. Sects. IV and V contain discussion and final conclusions.

II. MODEL

Suppose that a CCQE interaction occurred on a nucleon inside a nucleus, one nucleon is knocked out and detected together with a final state muon. Suppose also that the target nucleus is at rest and no other particles are knocked out.

The energy and momentum conservation read:

$$E + M(A) = E' + E_{p'} + E_{A-1} \tag{3}$$

$$\vec{k} = \vec{k}' + \vec{p}' + \vec{p}_{A-1} \tag{4}$$

where $(E, \vec{k})$, $(E', \vec{k}')$ are the neutrino and muon four-momenta, $M(A)$ is the mass of target nucleus of atomic number A, $(E_{A-1}, \vec{p}_{A-1})$, $(E_{p'}, \vec{p}')$ are the final state nucleus and final state nucleon four-momenta.

In the IA picture, the interaction occurs on a nucleon with momentum $\vec{p}$. If no final state interactions took place, it must be that

$$\vec{p} = -\vec{p}_{A-1}. \tag{5}$$

This means that the initial nucleus state is factorized into a nucleon participating in the interaction and a spectator remnant nucleus with $A - 1$ nucleons.

We can decompose $\vec{p}$ into components parallel and perpendicular with respect to the neutrino direction, $\vec{k}$, which is assumed to be known:

$$\vec{p} = \vec{p}_L + \vec{p}_T \tag{6}$$

The same can be done with vectors $\vec{k}'$ and $\vec{p}'$. We get the following equations:

$$E + M(A) = E' + E_{p'} + E_{A-1} \tag{7}$$
$$E = k'_L + p'_L - p_L \tag{8}$$
$$0 = \vec{k}'_T + \vec{p}'_T - \vec{p}_T. \tag{9}$$

In this we use the fact that for the neutrino $|\vec{k}| = E$. p_L, k'_L and p'_L denote projections of the corresponding three vectors on the direction of $\vec{k}$.

The final state nucleus is in general in an excited state and its invariant mass is $M^*(A-1)$. If the final state muon and proton are measured, $\vec{p}_T$ is known and we obtain two equations for E and p_L that can be easily solved. We get:

$$p_L = \tfrac{1}{2}(M(A) + k'_L + p'_L - E' - E_{p'}) - \frac{p_T^2 + M^*(A-1)^2}{2(M(A) + k'_L + p'_L - E' - E_{p'})} \tag{10}$$

$$p_{rec} = \sqrt{\vec{p}_T^2 + p_L^2}, \tag{11}$$

$$E = k'_L + p'_L - p_L. \tag{12}$$

We notice that an analogous derivation can be calculated in the IA scheme treating a hit nucleon as a bound one with an unknown binding energy, neglecting initial and final state nuclei. The two derivations can be made completely equivalent if the binding energy is treated as nucleon momentum dependent.

We will not assume a constant average value of $M^*(A-1)$. Instead we introduce a probability distribution for the final state excitation energy using information about neutron occupancy in a given nucleus. In this paper, we will discuss ^{12}C and ^{40}Ar. In the case of argon, relevant information can be found in [24]. For the neutron separation energy, E, Gaussian distribution is assumed with central values E_α and standard deviation σ_α, see Table I.

For carbon, we used information about proton separation energies and widths from [6]. To summarize, we select a separation energy using the probability distribution

$$P(E) = \frac{1}{N}\sum_\alpha n_\alpha G(E - E_\alpha, \sigma_\alpha) \tag{13}$$

where n_α is the number of neutrons with separation energy E_α and N is the total number of neutrons

$$\sum_\alpha n_\alpha = N$$

and $G(x - x_0, \sigma)$ is a Gaussian distribution with mean value x_0 and standard deviation σ. The binding energies of carbon and argon nuclei in the ground state are respectively: $B = 92.16$ MeV and $B = 343.81$ MeV. It means that in the numerical computations for carbon, we assume

$$M(A) = 6M_n + 6M_p - 92.16 \text{ MeV},$$

$$M^*(A-1) = M(A) - M_n + E$$

where M_p and M_n denote proton and neutron masses, respectively. Analogous formulas are used for argon, with the values of 6, 6, and 92.16 replaced in the expression for $M(A)$ by 22, 18, and 343.81 respectively.

Subshell	E_α [MeV]	σ_α [MeV]	# neutrons n_α
$1s_{1/2}$	62	6.25	2
$1p_{3/2}$	40	3.75	4
$1p_{1/2}$	35	3.75	2
$1d_{5/2}$	18	1.25	6
$2s_{1/2}$	13.15	1	2
$1d_{3/2}$	11.45	0.75	4
$1f_{7/2}$	5.56	0.75	2

TABLE I. Neutron shell structure in ^{40}Ar [24]

Subshell	E_α [MeV]	σ_α [MeV]	# neutrons n_α
$1s_{1/2}$	40.8	9.1	2
$1p_{3/2}$	20.3	5	4

TABLE II. Neutron shell structure in ^{12}C [6]

II.1. Monte Carlo generators

In our tests, we used three MC generators: GENIE [18], NEUT [19] and NuWro [20]. Their basic structure is similar, however they differ in many details that may play a role in the comparisons we performed.

In CCQE events, target neutrons are typically described with (local) Fermi gas model. GENIE uses Bodek-Ritchie modification of the Fermi gas with a large momentum tail added in the neutron momentum distribution accounting for nucleon-nucleon correlation effects [25]. One of the options in NuWro is to use spectral functions [26]. In this approach one distinguishes if an interaction occurs on a nucleon described by a shell model or on a nucleon forming a correlated pair. In the second case the existence of a correlated spectator nucleon is assumed, that also propagates through the nucleus.

Its initial momentum is postulated to be opposite (as a three-vector) to that of the interacting nucleon.

For resonant pion production (RES) events, NEUT and GENIE use the Rein-Sehgal model [27] with upgraded information about resonance properties. NEUT includes resonance interference effects and anisotropy of the distribution of pions resulting from Δ decays [28]. NuWro has a separate treatment of the Δ resonance with form factors fitted to experimental data. Heavier resonances are included only in an approximate way using quark-hadron duality arguments. All three MCs differ in the way in which the non-resonant background contribution is included. All three MCs account for the Δ in-medium self-energy [29] using different approximations. NuWro models Δ finite life-time inside nucleus.

All the generators treat more inelastic events (DIS) in a similar way [30]. The same model of the inclusive DIS cross section is used and then PYTHIA fragmentation routines produce the final states. The differences are in the values of some PYTHIA parameters and also in the kinematical region where this formalism is used. NuWro extends to $W = 1.6$ GeV while GENIE and NEUT only to 1.8 or 2.0 GeV with KNO scaling arguments [31] applied in the transition region.

In the versions of NEUT (v. 5.1.4.2) and GENIE GENIE (v. 2.8.6) used in this study two-body current ("MEC") events are not produced. NuWro uses the Nieves model [2] with a momentum transfer cut $q \leq 1.2$ GeV/c [32]. 85% of MEC events occur on proton-neutron pairs [33], and finite state nucleons are assigned momenta using a phase space model [34]. For argon, an effective model accounting for isospin asymmetry is used [35]. NEUT partially accounts for a lack of MEC with a large effective axial mass in CCQE events $M_A = 1.21$ GeV. Also, NEUT assumes that 20% of Δs re-interact with nucleons and no pions appear in the final state.

There are also some differences in the final state interactions models. For pions, NEUT and NuWro use the Oset model [36] which in the case of NEUT, was further fine tuned to pion-carbon cross section data [37]. GENIE uses an effective model assuming the pion absorption cross section to be a fixed fraction of the pion reaction cross section.

III. RESULTS

In this section, we discuss the performance of the proposed method to select a high CCQE purity sample from a sample of CC0π1p events. We did many tests with a variety of fluxes, targets and MC event generators. In all the examples we investigated the conclusions were similar.

Table III shows basic information about all the simulations that were tested. We select charged current events with no mesons and exactly one proton above the assumed detection threshold with the MiniBooNE, NuMI and T2K ν_μ fluxes. The targets we consider are carbon and argon. In the case of carbon, the proton threshold is taken to be 400 MeV/c. In the case of argon, there is more flexibility on how to define the one muon and one proton event sample. We considered two options: either a proton threshold at 400 MeV/c to allow for comparisons with carbon, or 200 MeV/c which is the lowest threshold one can expect to achieve in experiments such as MicroBooNE. We employ three different nuclear models - Fermi Gas (FG), Local Fermi Gas (LFG), and Spectral Function (SF). In all cases, protons below threshold are assumed to be undetectable.

Target	MC	Flux	model	proton thresh. [MeV/c]	QE-like fraction	CCQE purity
^{12}C	NuWro	MB	SF	400	36.3%	82.4%
^{12}C	NuWro	MB	LFG	400	40.5%	85.0%
^{12}C	NEUT	MB	FG	400	41.5%	90.9%
^{12}C	GENIE	MB	FG	400	30.4%	91.3%
^{12}C	NEUT	T2K	FG	400	39.8%	91.5%
^{12}C	GENIE	NuMI	FG	400	10.0%	78.3%
^{40}Ar	NuWro	MB	LFG	400	39.0%	80.2%
^{40}Ar	NuWro	MB	SF	400	35.2%	77.3%
^{40}Ar	GENIE	MB	FG	400	29.1%	87.6%
^{40}Ar	NuWro	MB	LFG	200	39.0%	89.5%
^{40}Ar	NuWro	MB	SF	200	41.4%	88.5%
^{40}Ar	GENIE	MB	FG	200	37.3%	95.8%

TABLE III. Basic information about the MC simulations performed in this paper. See explanations in the text.

In the Table III the sixth column shows what fraction of CC events meet these initial CC0π1p criteria. In the last column the CCQE purity in the sample is shown. Differences seen in Table III for the same target and flux express a level of uncertainty in the models. For example in the case of the MB flux and carbon target the overall fraction according to GENIE is only $\sim$ 30% while according to NEUT and GENIE it is much larger, about 40%. This is because GENIE predicts a lower average proton momentum and fewer events pass the 400 MeV/c threshold. As for the CCQE purity, the NuWro results (lower purity) are probably more reliable because MEC events are included in the simulation. Fermi gas/SF differences can be explained by the fact that SF predicts a smaller CCQE cross section [38]. For the T2K flux, numbers are similar to MB, while for the NuMI flux with an average energy of $\sim$ 3 GeV there are many more inelastic events, typically with many pions, so the subsample of events with no mesons and only one visible proton is much smaller.

As an illustration for the numbers shown in Table III we present in Table IV more details about the NuWro simulations with the MB flux and carbon target. It should be stressed that in the case of MEC events the numbers in the last two columns depend on assumptions in the MEC hadronic model that are rather uncertain. We performed an analogous study using NEUT and obtained consistent results for the dominant CCQE contri-

bution.

Mode	CC	CC0π1p	>0 protons > 400MeV/c	exactly 1 proton > 400MeV/c
CCQE	51.5%	50.2%	35.7%	34.1%
RES	34.0%	5.0%	4.7%	3.1%
MEC	10.1%	9.8%	7.7%	3.3%
				=40.5%

TABLE IV. Breakdown of NuWro (LFG) signal events into interaction modes in a simulation using the MB flux and carbon target.

III.1. Reconstructed Initial Neutron Momentum

The reconstructed initial state neutron distributions, p_{rec} (see Eq. 11), for multiple nuclear models are shown in Fig. 1. We clearly see the typical shape of the nucleon momentum distributions from different models implemented in the MCs with a peak at $\sim 200-250$ MeV/c. In addition there is always a long tail extending to larger values of reconstructed neutron momentum. In Fig. 2, the reconstructed neutron momentum distribution is shown for the GENIE generator, using the NuMI ν_μ on-axis flux. Again the target nucleus is carbon. Here, we show contributions from CCQE and non-CCQE events separately. It can be clearly seen that the non-CCQE contribution is largely above the Fermi momentum, while true QE events are usually below the Fermi momentum. Similar structure was obtained in all the examples we considered. We conclude that imposition of a cut on reconstructed neutron momentum p_{rec} and rejection of events with large values of p_{rec} should select a high purity sample of CCQE events.

III.2. Cut optimization

The level of signal - background separation is found to be very good across all samples tested. Typical results are shown in Figs 3 and 4. They present curves of signal (true CCQE) acceptance vs background (true non-CCQE) rejection as a function of a cut on the reconstructed neutron momentum. Each point on the curves corresponds to a value of reconstructed neutron momentum cut.

In Fig. 4, we can see that the lower threshold degrades selection performance. It may be beneficial to impose a non-minimal threshold for protons, though this would also impact the available statistics.

The performance does not vary much as variables such as the generator, target nucleus, and proton tracking threshold, are changed. Most of the curves allow for over 80% signal acceptance with over 80% background rejection.

Our studies suggest that a cut at 300 MeV/c reconstructed neutron momentum provides the best performance in terms of efficiency and purity, though detector resolution effects may slightly modify this conclusion.

In Table V, we show the effect of the cut at $p_{rec} =$ 300 MeV/c on the simulated samples of events presented in Table III. In all the situations one obtains a sample with a purity of $\sim 95\%$, in several cases even better. As we will see in the next section for this sample of events the neutrino energy is reconstructed with very good precision.

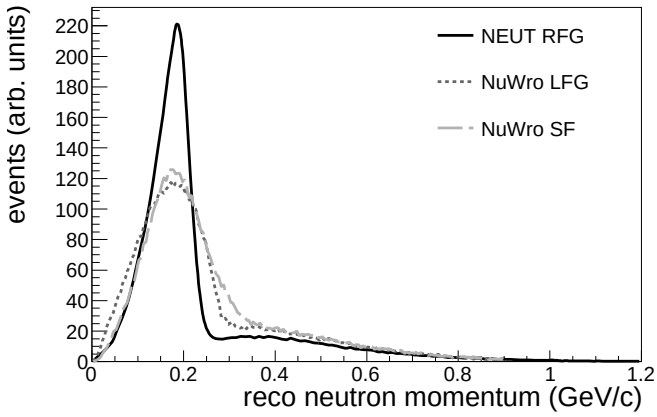

FIG. 1. Reconstructed initial state neutron momentum from one muon and one proton events for the global Relativistic Fermi Gas (RFG), Local Fermi Gas (LFG), and Spectral Function (SF) nuclear models. The target nucleus is carbon, and the incident neutrino flux is the MiniBooNE ν_μ flux. NEUT is used to produce the RFG simulation, while NuWro is used for LFG and SF samples. Each sample is normalized to have the same area.

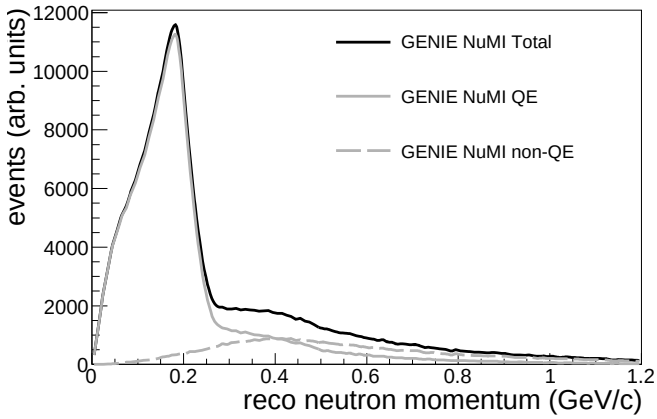

FIG. 2. Reconstructed initial state neutron momentum assuming the default GENIE RFG model. The target nucleus is carbon, and the incident neutrino flux is the NuMI on-axis ν_μ flux. Contributions from CCQE events and non-CCQE events are shown separately.

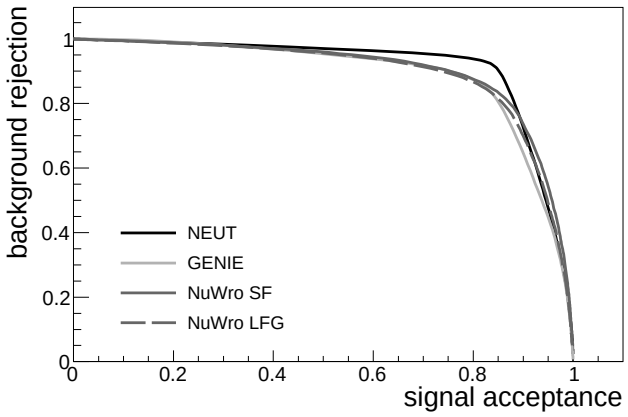

FIG. 3. Signal acceptance fraction vs background rejection fraction as a function of the cut on reconstructed neutron momentum for CC0π1p events. Shown are the default configurations of NEUT (solid black) and GENIE (solid light gray), as well as NuWro with a local Fermi Gas model (solid dark gray) and the Spectral Function model (dashed dark gray). In all cases, the target nucleus is carbon and the MiniBooNE ν_μ flux is used.

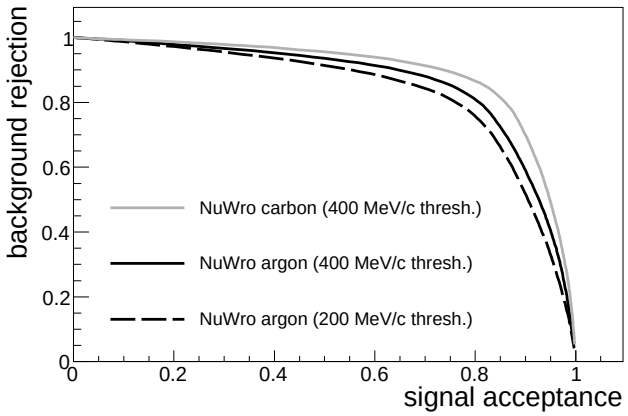

FIG. 4. Signal acceptance fraction vs background rejection fraction as a function of a cut on the reconstructed neutron momentum. Shown are predictions from NuWro for both carbon (solid gray) and argon (solid black) assuming a 400 MeV/c proton tracking threshold, and for argon also a curve assuming a lower proton tracking threshold of 200 MeV/c (dashed black).

III.3. Energy Reconstruction

Often, the neutrino energy is reconstructed using information from the final state muon only. Under the assumption that the target neutron is at rest and using energy and momentum conservation (in a similar way to that presented in Sec. II) one obtains

Target	MC	Flux	model	threshold [MeV/c]	overall fraction	CCQE purity
^{12}C	NuWro	MB	SF	400	26.7%	96.0%
^{12}C	NuWro	MB	LFG	400	31.8%	95.5%
^{12}C	NEUT	MB	FG	400	33.5%	98.2%
^{12}C	GENIE	MB	FG	400	24.7%	97.4%
^{12}C	NEUT	T2K	FG	400	32.5%	98.5%
^{12}C	GENIE	NuMI	FG	400	7.0%	95.3%
^{40}Ar	NuWro	MB	LFG	400	27.3%	94.7%
^{40}Ar	NuWro	MB	SF	400	23.2%	93.5%
^{40}Ar	GENIE	MB	FG	400	21.5%	96.3%
^{40}Ar	NuWro	MB	LFG	200	33.2%	96.6%
^{40}Ar	NuWro	MB	SF	200	30.3%	96.3%
^{40}Ar	GENIE	MB	FG	200	28.9%	98.7%

TABLE V. Values of selection efficiency (fraction of true CC events selected) and CCQE purity for different generators, targets, and models. The difference with respect to table III is that now a $p_{rec} < 300$ MeV/c cut is imposed.

$$E_{CCQE} = \frac{M_p^2 - m^2 + 2E'\tilde{M}_n - \tilde{M}_n^2}{2(\tilde{M}_n - E' + k'\cos\theta_\mu)} \qquad (14)$$

where M_p, M_n are the proton and neutron masses, $\tilde{M}_n = M_n - B$ with B binding energy, m is the muon mass, θ_μ is the angle of the muon with respect to the incoming neutrino direction.

When the hadronic final state can be reconstructed, neutrino energy reconstruction usually relies on the hadronic energy deposited in the detector - the exact details depend on the detector technology. In this case corrections must be made according to MC predictions for the amount of energy carried away by neutrons and the residual nucleus, or particles below threshold.

For events with the topology identified here, a cut on the neutron momentum has been shown to select a high purity sample of CCQE events which are either free from FSI or where FSI effects are weak. For these events, the neutrino energy can be accurately reconstructed with far less concern for missing energy.

Fig. 5 shows the difference between the true and reconstructed neutrino energy for a sample of CC0π1p events discussed in this paper, using our method (Eq. 12) with and without a cut on the reconstructed neutron momentum of 300 MeV/c. The cut removes most of events with poorly reconstructed neutrino energy, leaving a sample of events with neutrino energies reconstructed within 100 MeV of the true neutrino energy, with well over 90% of events energies reconstructed to better than 40 MeV of the true energy. Characteristic shapes seen in Fig. 5 come from the probability distribution for neutron binding energy. They are present because in the simulations the Fermi gas model was used with no information about neutron energy levels. Of course, in a real experimental situation the structures will likely be washed out by detector smearing effects.

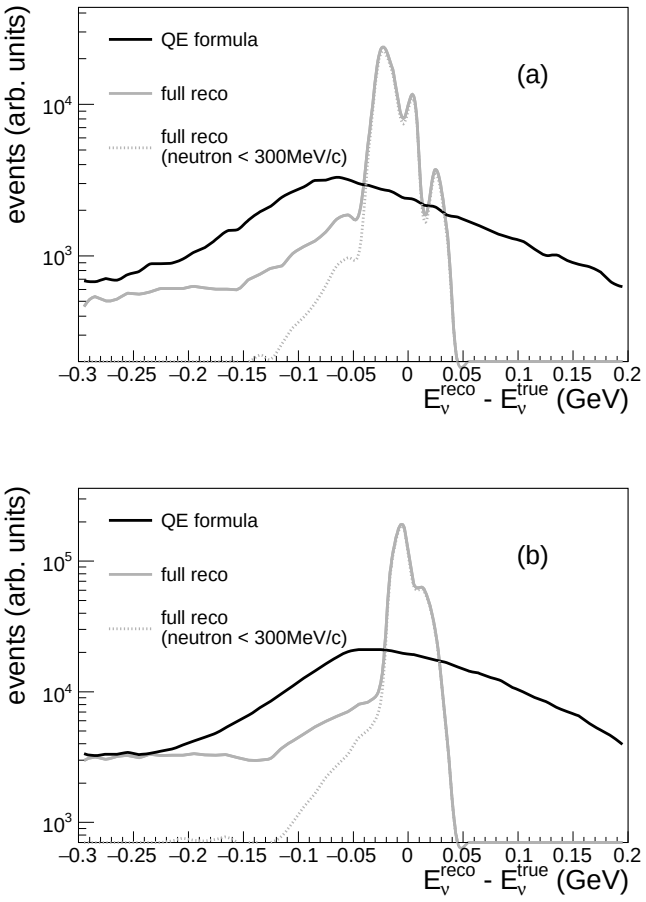

FIG. 5. Neutrino energy resolution for CC0π1p events, using the CCQE formula (black solid), the method proposed in this paper without (gray solid), and with a cut on the reconstructed neutron momentum at 300MeV/c (gray dotted). The target nucleus used is argon (a) or carbon (b) and the beam is MiniBooNE's ν_μ (a) and NuMI's on-axis ν_μ (b). The generator used is GENIE.

It is interesting to observe that FSI tends to lower the energy of final state particles, leading to the appearance of a tail of events being reconstructed with the energy often much smaller than the true one. Placing a cut at 300 MeV/c reconstructed neutron momentum reduces this tail significantly.

The solid line denotes a performance of the energy reconstruction based on Eq. (14). The method proposed in this paper is dramatically better.

IV. DISCUSSION

In the case of argon target with a very low proton detection threshold, there are many strategies in which one can obtain even better CCQE purity. For example, one can select events with exactly one proton above 400 MeV/c and also require there is no additional proton above 200 MeV/c. This is a more restrictive sample than discussed before as there are events with one proton above 400 MeV/c and a subleading proton between 200 and 400 MeV/c. According to NuWro with SF and the MiniBooNE flux, the sample of events defined in this way contains $\sim 27.7\%$ of the overall number of CC events. CCQE purity of this sample is 88.4%. A cut of the reconstructed neutron momentum at 300 MeV/c reduces this sample to $\sim 21.3\%$ of CC events with the purity as high as $\sim 97.1\%$. According to simulations done with LFG the purity of the selected sample is very similar: $\sim 97.7\%$.

An interesting question is if the cut on reconstructed neutron momentum discussed in this paper can tell us about RES and MEC events separately. We looked at the distributions of neutron momentum resulting from RES and MEC events in NuWro simulations with MB beam on the carbon target. RES events give rise to a very flat distribution of reconstructed momenta while MEC events show more structure: a gentle maximum at ~ 450 MeV/c with a wide spread. However, in both cases the results depend on several assumptions with large uncertainties and we think it may be problematic to try to use this technique to get information about the size of MEC contribution.

In a real experimental set up, the target is never pure carbon but usually CH or CH_2. In such a case, our conclusion about the CCQE purity of the selected sample remains valid as neutrino interactions on hydrogen cannot produce a $\mu^- + p$ final state. The only difference is in the relative normalization of the selected sample. It is smaller and the size of the difference will depend on neutrino flux spectrum.

The technique proposed in this paper selects CCQE interactions based on a lepton+proton topology with a kinematic cut. It is therefore not applicable to antineutrinos because for the CCQE reaction, there is a neutron in the final state rather than a proton and typically the neutron is very difficult to detect. This limits the applicability of our approach in CP violation studies using beams of both neutrinos and antineutrinos.

This technique is also not applicable to Cherenkov detector such as in the T2K far detector as most protons are below Cherenkov threshold and therefore are not detectable. However, it may be applied, for example, in the T2K near detector or in NOvA to improve understanding of the mapping between lepton kinematics and neutrino energy. It is most applicable to oscillation experiments with a detector capable of observing final state protons such as in a liquid argon TPC or a scintillator tracking detector.

We have not studied any effects caused by uncertainty of the incoming neutrino direction. For on-axis experiments, or detectors far from the beam source, this is less of a concern than for off-axis experiments close to the source.

V. CONCLUSIONS

We propose a method to select a high purity sample of muon neutrino CCQE scattering events. We checked the performance of the method using different neutrino fluxes, targets and MC generators. In all the cases the conclusion is that the purity of the sample is $\sim 95\%$. We also showed that for these events the neutrino energy can be reconstructed with a precision of around $30-40$ MeV (3-4% at 1 GeV). This is significantly better than using the "QE assumption" using only the lepton, and also an improvement on calorimetric energy reconstruction, removing the long tails of poorly reconstructed energies. This energy reconstruction could be useful for future neutrino oscillation experiments.

ACKNOWLEDGMENTS

JTS was supported by Fermilab Neutrino Physics Center Fellowship and also by NCN grant UMO-2014/14/M/ST2/00850. APF was supported by the UK Science and Technology Funding Council, and also by the Fermilab Intensity Frontier Fellowship. Fermilab is operated by Fermi Research Alliance, LLC under Contract No. DE-AC02-07CH11359 with the United States Department of Energy.

[1] A. A. Aguilar-Arevalo *et al.* [MiniBooNE Collaboration], Phys. Rev. D **81**, 092005 (2010).
[2] M. Martini, M. Ericson, G. Chanfray, and J. Marteau, Phys. Rev. C **80**, 065501 (2009); J. Nieves, I. Ruiz Simo, and M. J. Vicente Vacas, *ibid.* **83**, 045501 (2011).
[3] M. Martini, M. Ericson, and G. Chanfray, Phys. Rev. D **85**, 093012 (2012); O. Lalakulich, U. Mosel, and K. Gallmeister, Phys. Rev. **C86**, 054606 (2012); J. Nieves, F. Sanchez, I. Ruiz Simo, and M. J. Vicente Vacas, *ibid.* **D85**, 113008 (2012).
[4] J. G. Morfin, J. Nieves, and J. T. Sobczyk, Adv. High Energy Phys. **2012**, 934597 (2012); L. Alvarez-Ruso, Y. Hayato, and J. Nieves, New J. Phys. **16**, 075015 (2014).
[5] O. Benhar, N. Farina, H. Nakamura, M. Sakuda, and R. Seki, Phys. Rev. D **72**, 053005 (2005).
[6] S. Frullani and J. Mougey, Adv. Nucl. Phys. **14**, 1 (1984).
[7] P. A. Rodrigues *et al.* (MINERvA), Phys. Rev. Lett. **116**, 071802 (2016).
[8] K. Abe *et al.* (T2K), Phys. Rev. **D93**, 112012 (2016).
[9] H. Gallagher and Y. Hayato (Particle Data Group), Chin. Phys. **C38**, 090001 (2014).
[10] T. Walton *et al.* (MINERvA), Phys. Rev. **D91**, 071301 (2015).
[11] K. Garrow *et al.*, Phys. Rev. **C66**, 044613 (2002).
[12] G. Garino *et al.*, Phys. Rev. **C45**, 780 (1992); T. G. O'Neill *et al.*, Phys. Lett. **B351**, 87 (1995); O. Hen *et al.* (CLAS), *ibid.* **B722**, 63 (2013).
[13] U. Mosel, O. Lalakulich, and K. Gallmeister, Phys. Rev. Lett. **112**, 151802 (2014).
[14] X. G. Lu, L. Pickering, S. Dolan, G. Barr, D. Coplowe, Y. Uchida, D. Wark, M. O. Wascko, A. Weber, and T. Yuan, Phys. Rev. **C94**, 015503 (2016); X. G. Lu and M. Betancourt (MINERvA), in *27th International Conference on Neutrino Physics and Astrophysics (Neutrino 2016) (Neutrino 2016) London, UK, July 4-9, 2016* (2016).
[15] O. Benhar, A. Fabrocini, S. Fantoni, and I. Sick, Nucl. Phys. A **579**, 493 (1994).
[16] O. Hen *et al.*, Science **346**, 614 (2014).
[17] O. Benhar, D. Day, and I. Sick, Rev. Mod. Phys. **80**, 189 (2008).
[18] C. Andreopoulos, A. Bell, D. Bhattacharya, F. Cavanna, J. Dobson, *et al.*, Nucl. Instrum. Meth. **A614**, 87 (2010).
[19] Y. Hayato, Acta Phys. Polon. **B40**, 2477 (2009).
[20] T. Golan, C. Juszczak, and J. T. Sobczyk, Phys. Rev. C **86**, 015505 (2012).
[21] A. A. Aguilar-Arevalo *et al.* (MiniBooNE), Phys. Rev. **D79**, 072002 (2009).
[22] K. Abe *et al.* (T2K), Phys. Rev. **D87**, 012001 (2013), [Addendum: Phys. Rev.D87,no.1,019902(2013)].
[23] C. L. McGivern *et al.* (MINERvA Collaboration), Phys. Rev. D **94**, 052005 (2016).
[24] A. M. Ankowski and J. T. Sobczyk, Phys. Rev. C **77**, 044311 (2008).
[25] A. Bodek and J. L. Ritchie, Phys. Rev. **D23**, 1070 (1981).
[26] O. Benhar, A. Fabrocini, and S. Fantoni, Nucl. Phys. A **505**, 267 (1989).
[27] D. Rein and L. M. Sehgal, Annals Phys. **133**, 79 (1981).
[28] G. M. Radecky, V. E. Barnes, D. D. Carmony, A. F. Garfinkel, M. Derrick, E. Fernandez, L. Hyman, and G. Levman *et al.*, Phys. Rev. D **26**, 3297 (1982), [Erratum-ibid. D **26** (1982) 3297]; S. J. Barish, M. Derrick, T. Dombeck, L. G. Hyman, K. Jaeger, B. Musgrave, P. Schreiner, and R. Singer *et al.*, *ibid.* **19**, 2521 (1979).
[29] E. Oset and L. L. Salcedo, Nucl. Phys. A **468**, 631 (1987).
[30] A. Bodek and U. K. Yang, Nucl. Phys. Proc. Suppl. **112**, 70 (2002).
[31] Z. Koba, H. B. Nielsen, and P. Olesen, Nucl. Phys. **B40**, 317 (1972).
[32] R. Gran, J. Nieves, F. Sanchez, and M. J. Vicente Vacas, Phys. Rev. **D88**, 113007 (2013).
[33] I. Ruiz Simo, J. E. Amaro, M. B. Barbaro, A. De Pace, J. A. Caballero, G. D. Megias, and T. W. Donnelly, Phys. Lett. **B762**, 124 (2016).
[34] J. T. Sobczyk, Phys. Rev. C **86**, 015504 (2012).
[35] J. Schwehr, D. Cherdack, and R. Gran, *GENIE implementation of IFIC Valencia model for QE-like 2p2h neutrino-nucleus cross section*, (2016), arXiv:1601.02038 [hep-ph].
[36] L. L. Salcedo, E. Oset, M. J. Vicente-Vacas, and C. Garcia-Recio, Nucl. Phys. A **484**, 557 (1988).
[37] P. de Perio, *Proceedings, 7th International Workshop on Neutrino-nucleus interactions in the few GeV region (NUINT 11): Dehradun, India, March 7-11, 2011*, AIP Conf. Proc. **1405**, 223 (2011).
[38] O. Benhar and D. Meloni, Nucl. Phys. **A789**, 379 (2007).